UCRL-JC-130058
Preprint

An In-Situ Nanoindentation Specimen Holder for a High-Voltage Transmission Electron Microscope

M. A. Wall and U. Dahmen

This paper was prepared for submittal to
14th International Congress on Electron Microscopy 1998
Cancun, Mexico
Aug. 31-Sept.4, 1998

September 17, 1998

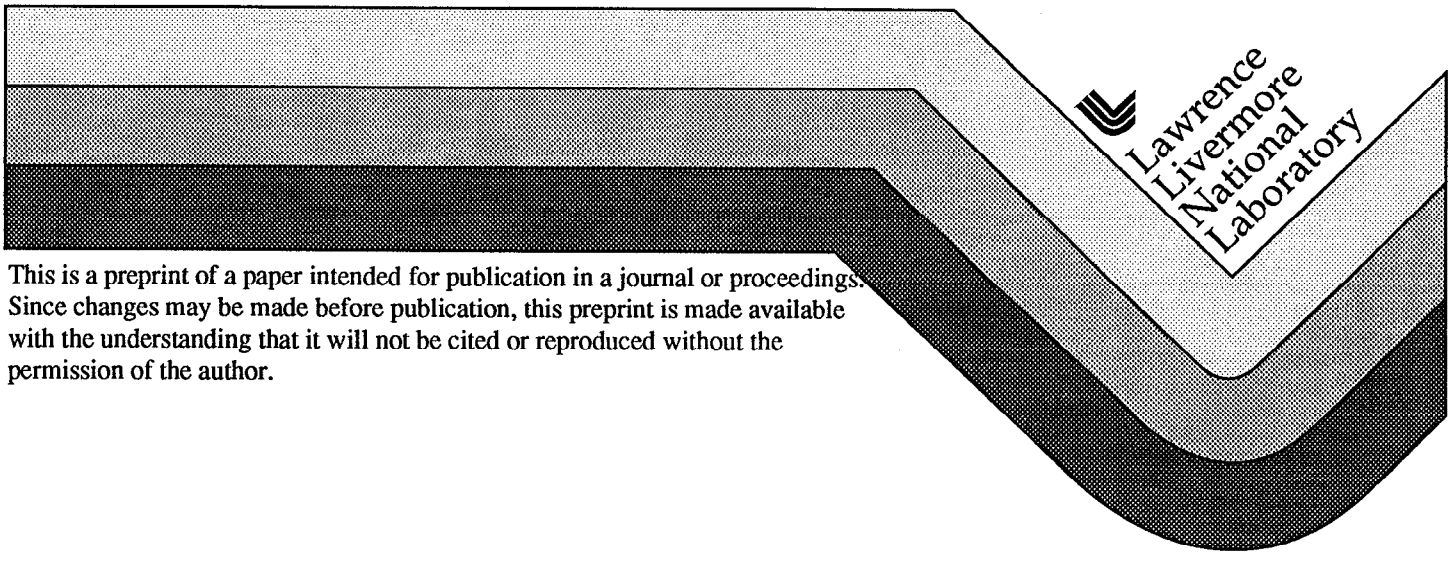

This is a preprint of a paper intended for publication in a journal or proceedings. Since changes may be made before publication, this preprint is made available with the understanding that it will not be cited or reproduced without the permission of the author.

DISCLAIMER

This document was prepared as an account of work sponsored by an agency of the United States Government. Neither the United States Government nor the University of California nor any of their employees, makes any warranty, express or implied, or assumes any legal liability or responsibility for the accuracy, completeness, or usefulness of any information, apparatus, product, or process disclosed, or represents that its use would not infringe privately owned rights. Reference herein to any specific commercial product, process, or service by trade name, trademark, manufacturer, or otherwise, does not necessarily constitute or imply its endorsement, recommendation, or favoring by the United States Government or the University of California. The views and opinions of authors expressed herein do not necessarily state or reflect those of the United States Government or the University of California, and shall not be used for advertising or product endorsement purposes.

An In-Situ Nanoindentation Specimen Holder for a High-Voltage Transmission Electron Microscope

M. A. Wall[1] and U. Dahmen[2]

Key words: Nanoindentation, cross-section, in situ, TEM

Abstract

This report describes the design, construction, and testing of a nanoindentation specimen holder used for dynamic observation of subsurface microstructure evolution under an indenter tip, while viewing in cross-section in a high-voltage transmission electron microscope (TEM). It also discusses the initial experimental results from in-situ indentation of Si samples in the TEM to demonstrate the capability of this new nanoindentation specimen holder, which uses three-axis position control of a diamond indenter in combination with micromachined specimens. Additionally, the sample design techniques developed for these procedures may eliminate the need for TEM specimen preparation in future ex-situ nanoindentation experiments and for sample preparation for characterizing these experiments in the electron microscope.

Introduction

Currently, there is a considerable amount of interest in the measurement of the mechanical properties (i.e., hardness, delamination, tribology) of nanostructured materials and in extremely small volumes, e.g., surfaces, single and multicomponent films, and nanosize particles. The invention and evolution of the nanoindentation instrument have greatly enhanced the progress of measuring the mechanical properties of nanostructured [1,2].

In many of the mechanical properties studies on nanostructured materials, the as-synthesized microstructure is typically characterized by microscopy and diffraction-related techniques. However, the deformed "site-specific" internal microstructure is often not characterized after mechanical testing. Examination of the "site-specific" internal microstructures often is not performed after nanoindentation because of the difficulty in preparing TEM samples. TEM replication and scanning electron and atomic force microscopy are often used to measure and observe the surface indent morphology. With any of these characterization approaches one can only attain an indirect conclusion regarding the internal microstructure response during indentation. Techniques such as micro-Raman spectroscopy [3] and resistivity [4] have been used to detect phase transformations within indents. However, the specific location within the indent volume, the volume fraction, and

[1] Chemistry and Materials Science Directorate, Lawrence Livermore National Laboratory (LLNL), 7000 East Avenue, Livermore, CA 94550.

crystallography of these new phases are in question and are often not retained after the indenter is removed.

A few published reports have characterized the post-indentation microstructure of nanoindents with TEM, which relates to our work on the indentation of Si [5,6]. These reports emphasize the importance of TEM characterization to the understanding of microstructural evolution effects such as elastic recovery, deformation mechanism, local fracture, and phase transformations. Nevertheless, these studies still showed specific, dynamic events measured in the typical load-displacement curve that might only be linked to a specific microstructure response by utilizing in-situ microscopy techniques.

Initially, the specimen holder demonstrated the capability of positioning a primitive sapphire tip onto the surface of a cleaved Si specimen and then indenting until fractured while viewing in cross-section [7,8]. Subsequently, several modifications were made to the specimen holder and new sample designs were employed using lithography techniques. This report discusses these latest developments and improved capabilities for in-situ nanoindentation experimentation.

Design and Construction Considerations

The basic design of the nanoindentation specimen holder employs several engineering features to enable the performance of in-situ nanoindentation and to offer flexibility in its design, making it possible to experiment with three-axis positioning of an object or device in a specific area on or about a specimen. These design features are as follows: (1) Large range of motion in combination with the nanometer scale resolution. (2) The indenter tip is on a removable mount so that tips or any other devices can be attached to the mount outside of the specimen holder. (3) Incorporation of a removable specimen mount with two-axis positioning capability for pre-alignment of the specimen with the indenter tip under an optical stereoscope.

Figure 1 is a schematic illustrating the general design and construction requirements employed to achieve our goal of in-situ nanoindentation experiments. As shown, a long stiff rod runs the length of the specimen holder and both pivots and slides about a universal four-point bearing surface yielding a lever arm reduction in lateral motion of approximately 10:1. One end of the rod passes through a bellows assembly and is attached to an ultra-low reduction gear motor drive for in-and-out (z axis) control. In series with this drive is a piezo stack for z axis indentation, which is located on the vacuum side of the bellows. The rear portion of the bellows assembly and z axis positioning motor is allowed to slide laterally across three adjustable nylon points that are co-planer. During lateral motion the bellows assembly is held

[2] National Center for Electron Microscopy, Lawrence Berkeley Laboratory, 1 Cyclotron Road, Berkeley, CA 94720.

in place by vacuum and the natural spring of the bellows . Screw piezos, having high resolution and large range of motion, are used to push on this bellows assembly for the x and y axis positioning. Return springs push back on the piezo drives for reverse motion. The diamond indenter is a three-sided, 30-degree pyramid and is boron-doped to eliminate charging under the electron beam.

We performed a number of test experiments to determine the repeatable specifications of the specimen holder. Based on these experiments, the current specifications are as follows: The z direction gear motor drive ranges from ±2.5 mm with a minimum step of ≤10 nm. The z direction gear motor can indent at a minimum constant displacement rate of ≈20 nm/sec. The z direction piezo has a range of ≈0.5 μm and a resolution of <0.2 nm. The lateral positioning screw piezo drives have a range and resolution of ±0.2 mm and ≤5.0 nm, respectively. There is currently no force measurement capability during an indenting experiment, therefore, work is in progress to develop this capability. Figure 2 shows the current configuration of the specimen holder.

Sample Design

We considered several methods to prepare specimens for in-situ indenting experiments. For test experiments, cleaving of the of Si wafers was fast and simple but these specimens proved mechanically unstable during indentation and their geometry was uneven. For controlled experiments, well-defined surface areas and volumes would be needed. To fabricate samples, we used standard lithographic and etching techniques. Figure 3(a) shows a series of small mesas on a larger single mesa. When turned on edge, these mesas are effectively a cross-section sample of the original Si wafer surface and the width becomes the viewing direction thickness in the TEM. As etched, the mesa dimensions typically range from 2 to 6 μm long × 1 to 4 μm wide × 2 μm deep. The wafer is then diced into 2 × 4 mm slices, each containing a single row of many mesas. The Si wafer is [110] oriented with the shape of the mesa being defined by [–110], [–111], and [1–11] planes, see Figure 3(b).

Experimental Procedures

The Si specimen is bonded to the specimen mount with epoxy. Then the specimen mount is positioned in the tip of the specimen holder. The indenter tip is moved along the z axis with the gear motor drive until it is within ≈0.5 mm of the Si sample. The Si sample mount can then be repositioned vertically (y axis) and laterally (x axis) so that the mesas are within ±0.2 mm of alignment with the indenter. The specimen holder is then ready for insertion into the electron

microscope. Once a mesa is located and oriented for TEM observation, the indenter tip is translated on the x and z axis until it appears close to the mesa to be indented. Then, the most tedious step can be performed, which is the alignment of the tip along the direction of the electron beam (y axis). First the indenter tip is moved towards the side of the mesa and just past the indenting surface ($+z$ direction). While the indenter tip is moved in the plus or minus y direction, the amount of focus change between the mesa and the tip is measured (i.e., focus steps). If the amount of focus change becomes less while moving the tip then the tip is moving closer to the mesa, or it is moving farther away. This defocus procedure will get the tip to within ≈ 1 μm of the mesa. With continued slow translation of the tip towards the mesa, the side of the indenter tip will eventually just touch the mesa. Because the (111) plane sides of the mesa are tapered the indenter tip is now in alignment at the center of the thickness of the mesa. Indenting using the piezo or the drive motor may begin after retracting the indenter tip ($-z$) and translating to the lateral center (x axis).

Experimental Results

Several test indentation experiments have been performed to date to determine the best experimental procedure, to assess the capability of the specimen holder, and to observe at a fundamental level the microstructural evolution of Si under the indenter tip. Figures 4 and 5 are micrographs and video recording frames of two in-situ experiments. In Figure 4(a), the diamond indenter tip is aligned with a 1.5-μm-thick $\times$ 4.0-μm-wide mesa and positioned within 1–2 nm of the surface. In Figure 4(b), the diamond tip is indented to a depth of $\approx$10 nm, the elastic response of the Si is clearly observed by the creation and motion of bend contours in the image. A large bend contour with a radius of approximately 0.15 μm is seen in the Si below and relatively centered under the indenter tip. At this point, there is no indication that dislocations or cracks have nucleated in the bulk Si. With continued indentation to a depth of $\approx$40 nm [Figure 4(c)], a larger crack has nucleated and propagated directly under the indenter. There is considerably more elastic strain as seen by the rapidly changing diffracting conditions around the indent. Again, there are no obvious signs of dislocations. With continued indenting to a final depth of $\approx$80 nm [Figure 4(d)], we observe that the crack under the indenter tip continued to propagate deeper into the Si, and the bend contour has moved out to a radius of approximately 0.3 μm, which is the edge of the viewing area of the camera. Because there are no strong diffracting conditions near the indenter tip/Si interface, it is difficult to see if any other cracks exist, or even the possibility that a few dislocations exist. Upon removing the indenter tip, a considerable amount of elastic recovery is observed, as indicated by the reversal of motion of the bend contours. A minor amount of plastic response

is also seen. In Figure 4(e), the indenter is removed and there is a strong, permanent bend contour indicating residual elastic strain. A planar crack (or fault) is seen along with a few dislocations near the indent and the crack. In Figure 4(f), the indent is then reindented to a depth of 100 nm and then unloaded. Dislocation nucleation and motion under the indenter tip were observed as well as signs of small cracking. Additionally, plastic deformation was observed on the lateral portions of the indent at these depths.

During indentation several bursts of plastic deformation were observed. During these bursts, the indenter tip was still observed to move smoothly into the Si. Upon removal of the indenter tip from these deeper indents, a considerable amount of "reverse" deformation was observed in the form of dislocation activity (apparent nucleation and motion) and possibly minor cracking. After complete removal of the indenter, residual strain fields still existed as seen by the remaining bend contours. Residual dislocations were primarily localized around the Si/indent interface.

Figure 5 is an image of a completed, 0.1-μm-deep indentation. Again, during indentation crack nucleation and propagation below the indenter was observed. Dislocation nucleation and motion became more obvious towards greater depths of indentation. In this particular indent the asymmetrical shape of the tip interacting with the Si results in an asymmetrical density of dislocations around the indent.

We performed additional indents, some of which reached depths as great as 0.3 μm. At these depths, the Si mesa was typically destroyed by cracks propagating to its outer sides. Other indents were quite shallow. For an indent only 10-nm deep residual strain fields existed, presumably from permanent plastic deformation which was not resolved in detail in these experiments and again appears during unloading

Discussion

A number of engineering design approaches could have been used to construct this specimen holder. However, our experimental results demonstrate that the current design meets the criteria of having three-axis motion with good resolution and range. The specimen holder translates and tilts with little or no disturbance to the indenter tip and/or its position with respect to the specimen. There does not appear to be any drift of the indenter tip with respect to the specimen, although a small amount of vibration occurs during lateral positioning due to the rapid mechanical motion of the screw piezos. The specimen holder is flexible as demonstrated in experiments that deformed carbon nanotubes in-situ [9]. Basically, any micro-mechanical/electrical/magnetic device can be attached (accounting for size requirements) to the three-axis positioning rod and located on, or near, a specimen.

We believe that our results are the first direct observation of internal microstructure evolution and response during an indentation experiment. However, a complementary experiment on the in-situ observation of the bending of micro-machined Si wedges has also been reported [10].

We also compared our observations, regarding the characterization of after effects of nanoindents with TEM, with those of others [5]. At the onset of indentation in conventional indentation experiments, there is some concern with possible "surface flexure" which leads to an inaccurate indenter depth measurement. We did not observe sample motion on the scale of 1–2 nm, which would be the smallest detail that could be measured at the magnifications used in these experiments. However, we did observe the diffracting conditions in the crystalline diamond tip change during indentation, an indication of the elastic response of the diamond. It would be entirely possible to perform these indents at a much higher magnification to look for sample compliances other than the elastic response of the indenter and the region under the indenter.

After the initial indentation, through the elastic response zone and into the plastic deformation mode, cracking appears to be the first mode of deformation and not dislocation nucleation and motion. As noted, signs of intermittent bursts of plastic deformation are seen around the indenter, independent of larger cracking. However, the exact nature of this plastic deformation remains unclear. There are some signs of dislocations after unloading from deeper indents, but because of the highly strained material around the indenter during indentation, the diffraction imaging conditions for imaging of dislocations varies rapidly and/or are low in contrast. As described, the imaging conditions (i.e., bend contours) move periodically and then relax as the indenter moves farther into the Si, indicating a relaxation of stress by plastic deformation. Numerous reports suggest a phase transformation to a more dense phase occurs in Si and may account for the low dislocation density. Although a phase transformation cannot be ruled out, there is some suggestion of another mechanism that might explain the observation of the indenter moving into the Si with little dislocation activity. The tip of the indenter is not very smooth, therefore, as the tip region is moving into initial contact with the Si, the Si is trying to conform to the local (atomic scale) irregularities of the tip. As the tip continues to move past these local contact sites, the Si relieves the local stress through micro-cracking and cleaving. This action then allows for the possible ejection of the Si particles out of the indented region. Certainly, more experiments performed in the diffraction mode and at higher magnification in image mode are required to elucidate the exact nature of the microstructure under the indenter tip at these initial stages.

Similar to Page et al. [5], we did not observe any "pop-in" like behavior in Si during these experiments; but they did observe this behavior in sapphire. This in-situ TEM indentation technique may be a way of elucidating this type of phenomena.

In all of our deeper indents (greater than the tip radius, 50 nm), we observed a noticeable elastic recovery and plastic deformation in the form of dislocation nucleation during unloading. This may be the microstructural response, noted as "pushing the indenter upwards" or "reverse thrust". This microstructure response could also be explained by a phase transformation, as proposed in the literature. To date, it is not obvious in our experiments that any phase transformation occurs during indentation or upon removing the indenter. The indentation experiments are stable enough that these could be repeated in the diffraction mode to look for any new phases.

After indentation, we did not see an amorphous region in the center of the indent. For the small indents, it would be difficult to observe a low-contrast phase amorphous phase, primarily because the samples are up to 2 μm thick in the viewing direction. It should also be noted that the indents are not as deep and the tips are of a different geometry than those of Page et al. [5].

The design of the Si mesa samples appear to be very compatible with these experiments. Using lithography techniques, the samples can be produced in large numbers, they have a well-defined volume and crystallography (which would be necessary for potential modeling purposes), and they are directly observable in cross-section in the electron microscope without any additional preparatory procedures. We are also exploring the possibility of performing ex-situ nanoindentation experiments on these Si samples and then performing TEM observation, eliminating the need for site-specific sample preparation of the indents. This process would enable us to understand the mechanical response of these mesas as compared with the larger Si wafer surfaces and possibly a calibration for the loading during the in-situ experiments. We have also been successful in evaporating thin films onto these Si mesas, therefore, future in-situ experiments are planned for these films.

Conclusion

The results of these experiments and operational testing of the nanoindentation specimen holder offer an experimental procedure and instrument that is reproducible and flexible, and has the potential for yielding a multitude of unique in-situ observations in the high-voltage electron microscope. This is demonstrated in the first-direct observations of sub-surface microstructural evolution in Si under the indenter tip during indentation. Coupled with the future development of force measuring capability, the potential exists for the creation of a new area of quantifiable, in-situ, nanoscale mechanical deformation study. The modifications and

successful applications of the specimen holder in plastically deforming carbon nanotubes in-situ create the potential for many new types of in-situ experiments.

Acknowledgments

The authors gratefully acknowledge Richard Gross of LLNL and Doug Owen of LBL for their technical support. They also thank Mehdi Balooch of LLNL and Tim Weihs of Johns Hopkins University for their many discussions. This work was performed under the auspices of the US Department of Energy by the Lawrence Livermore National Laboratory under contract W-7405-Eng-48; and by the Director, Office of Energy Research, Office of Basic Energy Sciences, Materials Sciences Division of the US Department of Energy under Contract No. DE-AC03-76SF00098.

References

1. M. F. Doerner and W. D. Nix, "A method for interpreting the data from depth sensing indentation instruments," *J. of Mat. Res.* **1**, 601–609 (1986).

2. W. C. Oliver and G. M. Pharr, "An improved technique for determining hardness and elastic modulas using load and displacement sensing indentation experiments," *J. of Mat.* Res. **7**, 1564–1583 (1992).

3. A. Kailer, Y. G. Gogotsi, and K. G. Nickel, "Phase transformations of silicon by contact loading," *J. Appl. Phys.* **81**(7), 3057–3063 (1997).

4. I. V. Grdneva, Yu V. Milman, and V. I. Trefilov, "Phase transitions in diamond-structured crystals during harness measurement," *Phys. Status Solidi A* **14**, 177–182 (1972).

5. T. F. Page, W. C. Oliver, and C. J. McHargue, "The deformation and behavior of ceramic crystals subjected to very low load (nano)indentations," *J of Mat. Res.* **7**, 450–473 (1992).

6. D. L. Callahan and J. C. Morris, "The extent of phase transformation in Si hardness indentations," *J. of Mat. Res.* **7**, 1614–1617 (1992).

7. M. A. Wall and U. Dahmen, "Techniques for in-situ mechanical deformation of nanostructured materials," *Proc. Micros. Soc. Amer.* (Kansas City, MO, 1995) pp. 240–241.

8. M. A. Wall and U. Dahmen, "Development of an in-situ nanoindentation specimen holder for the high voltage electron microscope," *Proc. Micros. Soc. Amer.* (Cleveland, OH, 1997) pp. 593–594.

9. T. Scheng, 1997, private communication.

10. E. Langer and D. Katzer, "Dislocation emission from moving cracks in Si at room temperature," *J. of Mat. Sci. Let.* **17**, 1256–1257 (Sept 1, 13, 1994).

Figure 1. A schematic of the nanoindentation specimen holder.

Figure 2. Photograph of the nanoindentation specimen holder in its current configuration.

Figure 3. (a) Scanning electron micrograph of a row of small Si mesas on a larger single Si mesa. (b) Higher magnification of a 2×4 μm mesa.

Figure 4. The first four frames (a–d) are extracts from a video camera (e) and (f) are micrographs. (a) Alignment of a diamond indenter near the surface of a 1.5-μm-thick Si mesa prior to indentation. (b) Indentation to a depth of $\approx$10 nm, showing elastic response of the Si by the bend contour under the indenter tip. (c) Indentation to a depth of $\approx$50 nm precipitates a crack and increases the amount of elastic strain under the indenter tip. (d) Continued indentation to a depth of 80 nm increases the amount of elastic distortion and propagates the crack under the indenter tip. (e) Upon removal of the indenter, another planar fault or crack is visible as well as dislocations. (f) Re-indentation to a depth of $\approx$100 nm results in the creation of numerous small cracks, dislocations, and minor extrusion of Si above the surface.

Figure 5. Indent to a depth of $\approx$100 nm, showing visible cracks and dislocation in the area around the indent.

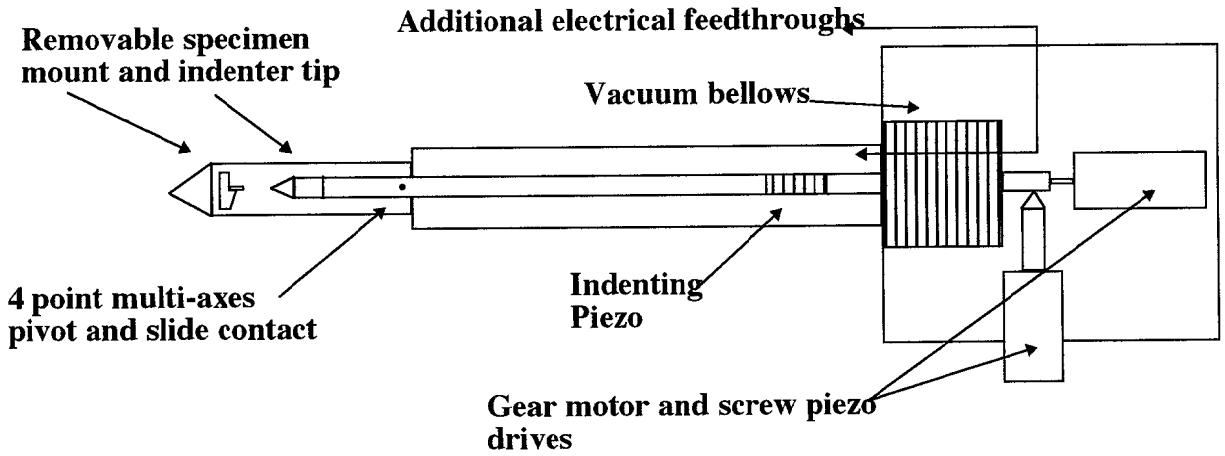
Removable specimen
mount and indenter tip
Additional electrical feedthroughs
Vacuum bellows
4 point multi-axes
pivot and slide contact
Indenting
Piezo
Gear motor and screw piezo
drives

Figure 1

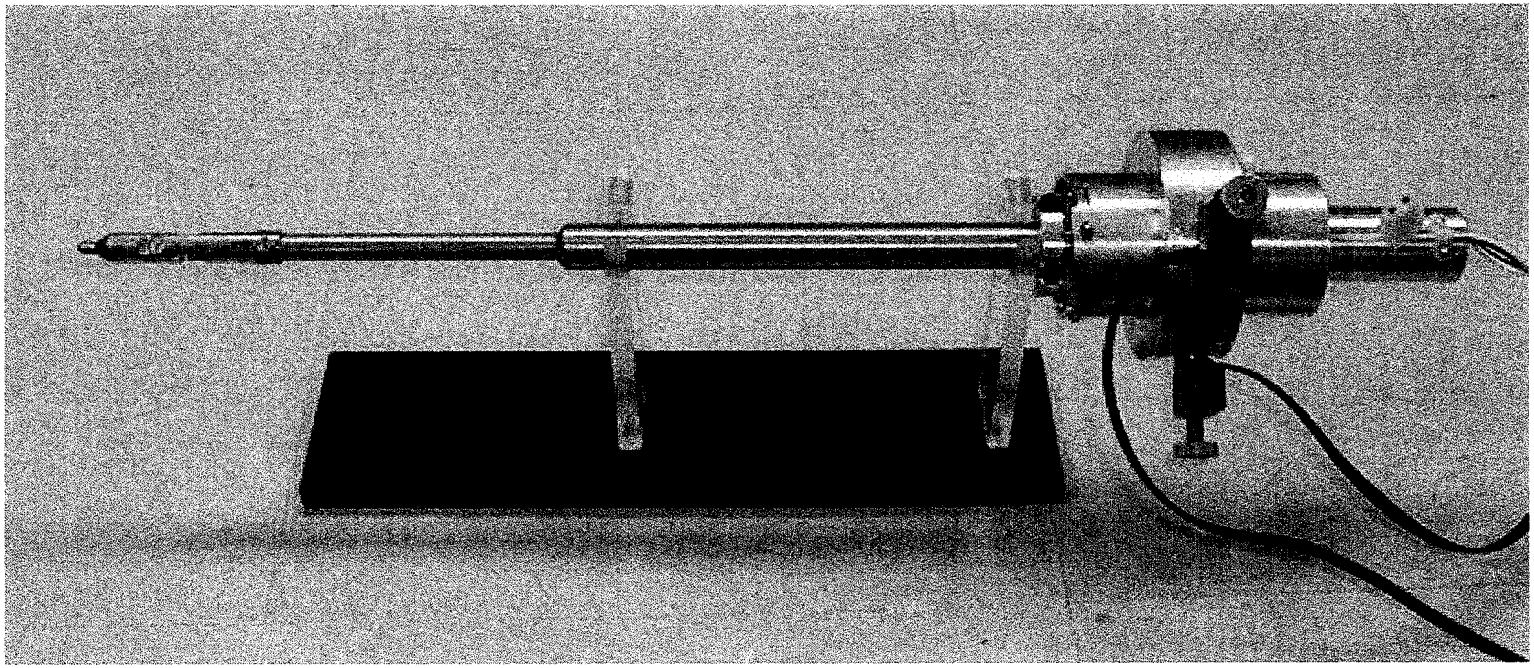

Figure 2

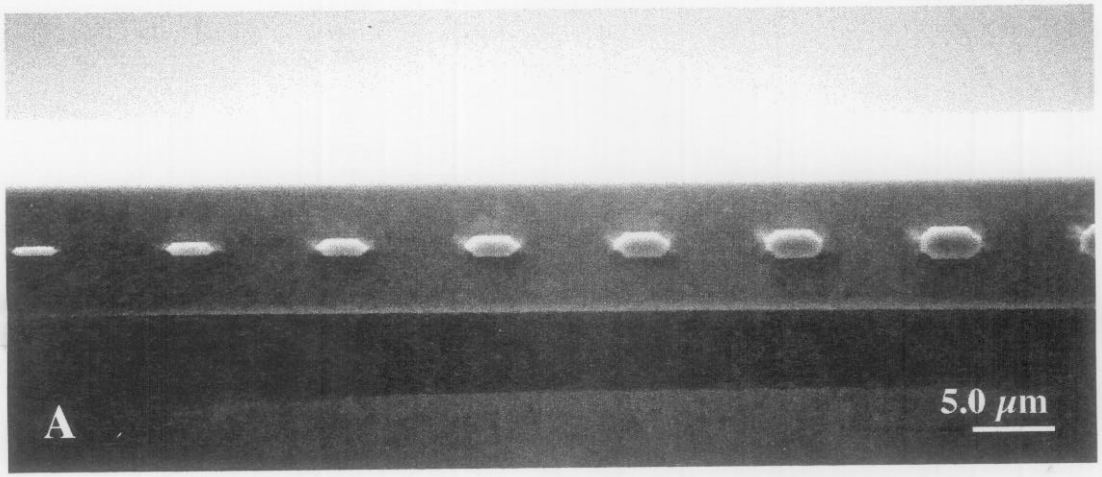

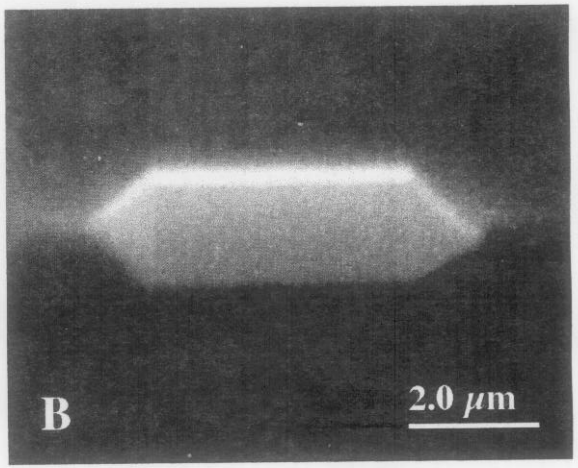

Figure 3

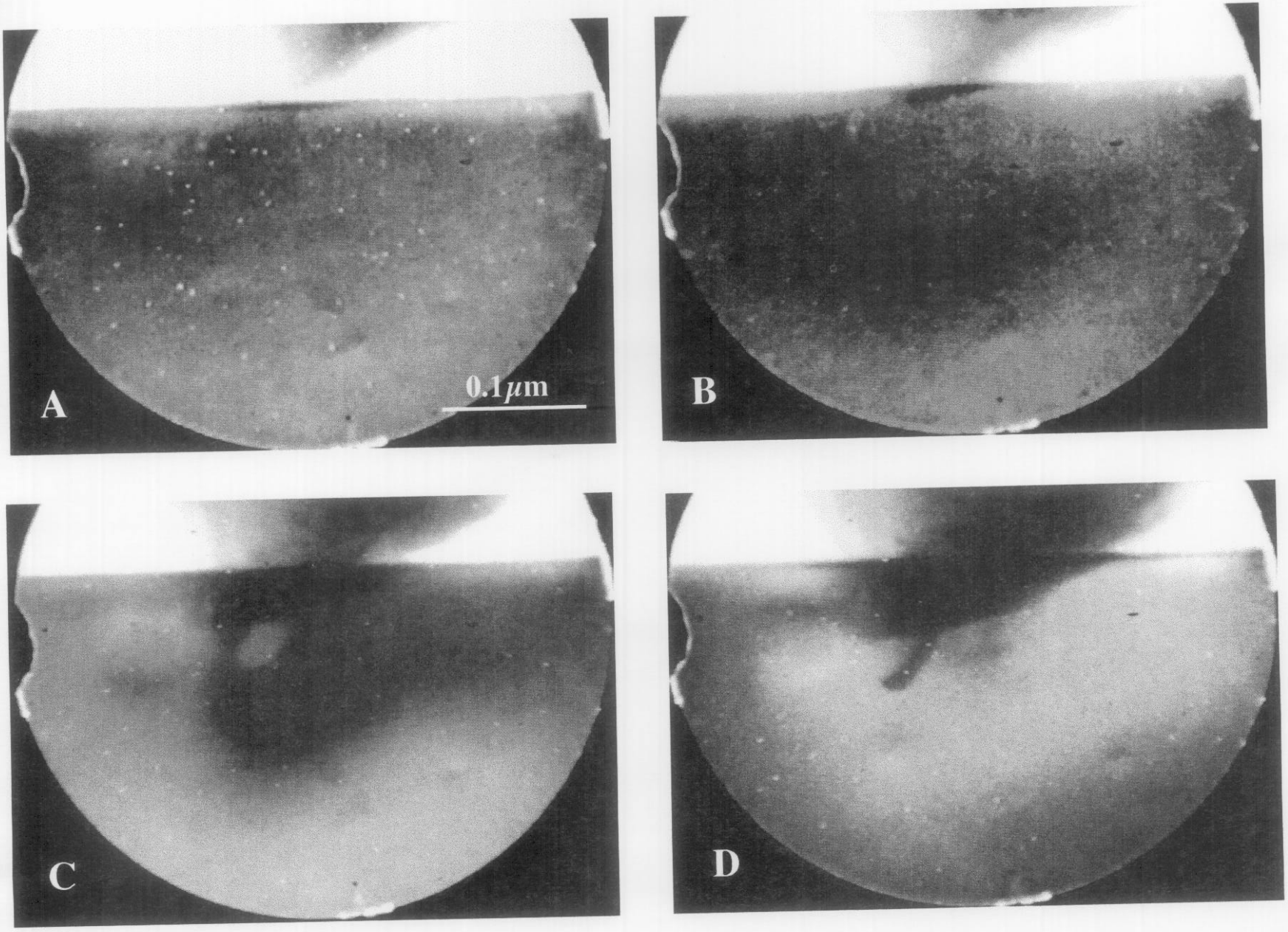

Figure 4

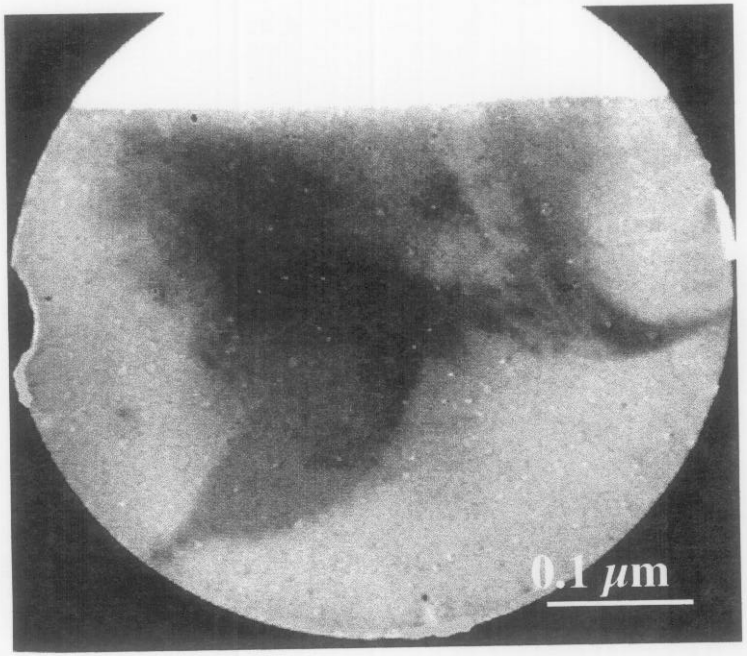

Figure 5